Full-wave Simulation of Finite-amplitude Ultrasound in Heterogeneous Media

Gianmarco Pinton
Biomedical Engineering
Duke University
Durham, North Carolina 27708–0281
Email: gfp@duke.edu

Gregg Trahey
Biomedical Engineering
Duke University
Durham, North Carolina 27708–0281

***Abstract*—A full-wave equation that describes nonlinear propagation in a heterogeneous attenuating medium is solved numerically with finite differences in the time domain (FDTD). Three dimensional solutions of the equation are verified with water tank measurements of a commercial diagnostic ultrasound transducer and are shown to be in excellent agreement in terms of the fundamental and harmonic acoustic fields, and the power spectrum at the focus. The linear and nonlinear components of the algorithm are also verified independently. In the linear non-attenuating regime solutions match results from Field II, a well established software package used in transducer modelling, to within 0.3 dB. Nonlinear plane wave propagation is shown to closely match results from the Galerkin method up to four times the fundamental frequency. In addition to thermoviscous attenuation we present a numerical solution of the relaxation attenuation laws that allows modelling of arbitrary frequency dependent attenuation, such as that observed in tissue. A perfectly matched layer (PML) is implemented at the boundaries with a novel numerical implemenation that allows the PML to be used with high order discretizations. A -78 dB reduction in the reflected amplitude is demonstrated. The numerical algorithm is used to simulate a diagnostic ultrasound pulse propagating through a histologically measured representation of human abdominal wall with spatial variation in the speed of sound, attenuation, nonlinearity, and density. An ultrasound image is created in silico using the same physical and algorithmic process used in an ultrasound scanner: a series of pulses are transmitted through heterogeneous scattering tissue and the received echoes are used in a delay-and-sum beamforming algorithm to generate a images. The resulting harmonic image exhibits characteristic improvement in lesion boundary definition and contrast when compared to the fundamental image. We demonstrate a mechanism of harmonic image quality improvement by showing that the harmonic point spread function is less senstive to reverberation clutter.**

I. Introduction

Characterization of acoustic waves that propagate nonlinearly in an inhomogeneous medium has important applications in diagnostic and therapeutic ultrasound. The heterogeneous composition of tissue distorts the phase and generates unwanted reverberation of an ultrasonic signal. This results in the degradation of the lateral resolution and contrast of an ultrasonic scanner. The nonlinearity of wave propagation is used to the advantage of diagnostic scanners that use the harmonic components of the ultrasonic signal to improve the resolution and penetration of clinical scanners [1]. Harmonic imaging has been shown to have an important effect in reducing phase aberration and clutter [2].

A number of equations and numerical methods that address nonlinear propagation, heterogeneous media, or multiple scattering have been proposed. Ultrasonic propagation through fine scale heterogeneities has been simulated with a finite difference time domain (FDTD) solution of the 3D linear wave equation [3]. The full-wave equation accounts for multiple reflections and scattering but current numerical implementations lack the ability to simulate nonlinear propagation and attenuation. The Khokhlov-Zabolotskaya-Kuznetsov (KZK) equation or nonlinear one-way parabolic wave equation, accounts for nonlinearity, attenuation, and diffraction within a paraxial approximation. The parabolic wave equation assumes that field variations transverse to the direction of propagation are slow compared to axial variations and the paraxial approximation limits the equation's validity to about 15° from the axis of propagation. Additionally this one-way wave equation does not model reflections, scattering, and heterogeneities. The nonlinear full-wave equation describes acoustic fields in a nonlinear thermoviscous medium. It has the advantages of both the three dimnensional linear wave equation and the nonlinear parbolic wave equation by incorporating nonlinearity, attenuation, and all wave effects, such as multiple scattering, reflection, and refraction. It is not limited by a paraxial approximation so it accurately describes an ultrasonic beam in the off axis region and it is valid for arbitrary scatterers in the field.

The incorporation of arbitrary frequency dependent absorption laws is straightforward in frequency domain methods. However it is numerically intractable for time-domain methods to solve the equivalent convolution. In this paper, in addition to thermoviscous attenuation, which is only valid for fluids, we use relaxation mechanisms to model arbitrary attenuation, such as the power laws observed in tissue. The numerical methods are based on research in seismic wave field but are adapted for the high order spatial discretizations used here.

Here we propose a novel three-dimensional numerical solution to a nonlinear full-wave equation that additionally describes arbitrary frequency dependent attenuation and variations in density. As the accuracy of simulations improves it becomes increasingly important to include higher order effects. We present the first numerical method that comprehensively

describes three dimensional nonlinear wave propagation in heterogenous media with arbitrary attenuation law. This paper also describes the implementation of perfectly matched layers (PML) at the boundaries to reduce reflections to negligible levels. It is shown that the FDTD method can accurately represent nonlinear ultrasonic propagation from a diagnostic transducer and that it can simulate heterogeneities in speed of sound, attenuation, nonlinearity, and density.

II. Methods

A. Acoustic Equation

The nonlinear full-wave equation used in this paper is a second order wave equation that describes a nonlinear wave propagating in an attenuating medium.

$$\nabla^2 p - \frac{1}{c_0^2}\frac{\partial^2 p}{\partial t^2} + \frac{\delta}{c_0^4}\frac{\partial^3 p}{\partial t^3} + \frac{\beta}{\rho c_0^4}\frac{\partial^2 p^2}{\partial t^2} + \frac{1}{\rho}\nabla p \cdot \nabla \rho - \sum_{m=1}^{v} \xi_m = 0 \tag{1}$$

where ξ_m satisfies the equation

$$\dot{\xi}_m + \omega_m \xi_m = a_m \omega_m \frac{\Delta c}{c_0} \nabla^2 p \tag{2}$$

The first two terms in Eq. 1 represent the linear wave equation, the third term accounts for thermoviscous diffusivity, followed by nonlinearity, variations in density, and v relaxation mechanisms. Here p is the acoustic pressure, c_0 and ρ are the equilibrium speed of sound and density, δ is the acoustic diffusivity, and β is the nonlinearity parameter. The nonlinear parameter B/A is related to the coefficient, β, by $\beta = 1 + B/2A$ and the diffusivity δ can be expressed as a function of the absorption coefficient α with the equation $\delta = 2\alpha c_0^3/\omega^2$ (where ω is the angular frequency). The material parameters c_0, δ, ρ and β can be functions of space. The relaxation equation (Eq. 2) has v peaks at characteristic frequencies ω_m with weight a_m that depend on the particular frequency dependent attenuation law that is being modeled. The change in speed of sound Δc must obey the Kramers-Kronig relation to preserve causality.

B. Diffraction

Explicit finite differences in the time domain are used to discretize the nonlinear full-wave equation on a three dimensional Cartesian grid. The three dimensional linear wave equation is modeled with a rotated stencil in Cartesian coordinates. Fourth order spatial derivatives were used to minimize the effects of numerical dispersion and reduce the requirements for grid refinement. Higher order discretizations that operate only in the Cartesian directions tend to have unwanted directionality– the wave propagates at different speeds along the direction of discretization compared to directions that are at an angle [4]. This type of error has particular significance for correct focusing and spherical propagation from point scatterers. To minimize this effect, the spatial discretization used here has two rotated stencils in addition to the conventional Cartesian stencil. The total star-shaped stencil for the spatial derivatives is shown below,

$$\begin{aligned}\nabla^2 p \approx\ & C_{i,j,k}^n = \\ & (1-\gamma-\eta) \sum_{|\theta|+|\phi|+|\psi|=1} \frac{-p^n_{i+2\theta,j+2\phi,k+2\psi} + 16p^n_{i+\theta,j+\phi,k+\psi} - 15p^n_{i,j,k}}{12(\Delta x^2 \delta_{1|\theta|} + \Delta y^2 \delta_{1|\phi|} + \Delta z^2 \delta_{1|\psi|})} \\ & + \gamma \sum_{|\theta|+|\phi|+|\psi|=2} \frac{-p^n_{i+2\theta,j+2\phi,k+2\psi} + 16p^n_{i+\theta,j+\phi,k+\psi} - 15p^n_{i,j,k}}{12(\Delta x^2 \delta_{1|\theta|} + \Delta y^2 \delta_{1|\phi|} + \Delta z^2 \delta_{1|\psi|})} \\ & + \eta \sum_{|\theta|+|\phi|+|\psi|=3} \frac{-p^n_{i+2\theta,j+2\phi,k+2\psi} + 16p^n_{i+\theta,j+\phi,k+\psi} - 15p^n_{i,j,k}}{12(\Delta x^2 \delta_{1|\theta|} + \Delta y^2 \delta_{1|\phi|} + \Delta z^2 \delta_{1|\psi|})}\end{aligned} \tag{3}$$

where $\theta,\ \phi,\ \psi$ have the possible values -1, 0, 1, and γ and η are arbitrary weighting coefficients with $\gamma + \eta \leq 1$, $\gamma \geq 0$, and $\eta \geq 0$, and, for this equation only, δ is the Kronecker delta function rather than the diffusivity.

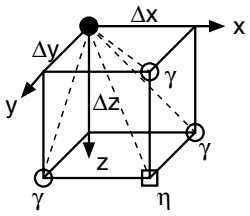

Fig. 1. Directions of the stencil for the linear wave equation in the positive quadrant.

The linear temporal derivatives are approximated by second order finite differences. The spatial derivatives in the density term are modeled with a standard fourth order approximation, but because only a first order derivative is being calculated the total width of the spatial stencil remains unchanged.

III. Results

The linear non-attenuating algorithm was compared to an equivalent Field II simulation for a commercial transducer. Field II solves the wave equation with the Tupholme-Stepanishen method for calculating linear pulsed ultrasound fields in a homogeneous medium. It has been widely validated and is commonly used to model transducers.

Figure 2 compares the intensity of the acoustic field for the Field II and FDTD nonlinear full-wave simulations across the lateral plane. The agreement is good throughout the simulated region. There are small visible differences, notably the -6 dB contour is approximately 1 mm more proximal to the transducer face in the nonlinear full-wave simulation and the -20 dB contour is slightly narrower at shallow depths ($z < 1.5$ cm). However, the overall morphology of the contours is very close.

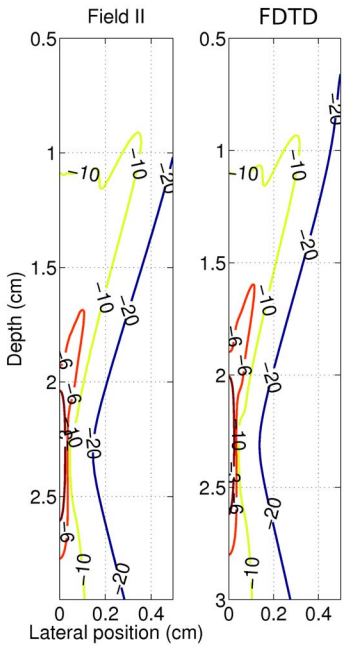

Fig. 2. A comparison of the intensity of the acoustic field as calculated by Field II and the linear inviscid FDTD nonlinear full-wave method for a commercial clinical ultrasound transducer. The lateral plane is shown.

A. Nonlinear plane wave

Results from the inviscid FDTD nonlinear full-wave simulation were compared to the results from the Galerkin method applied to the inviscid Burgers' equation. In the frequency domain (right graph of Fig. 3) there is excellent agreement at the fundamental and second harmonic frequencies. At the third harmonic there is a 1.2 dB difference between the peaks and at the fourth there is a 2.5 dB difference.

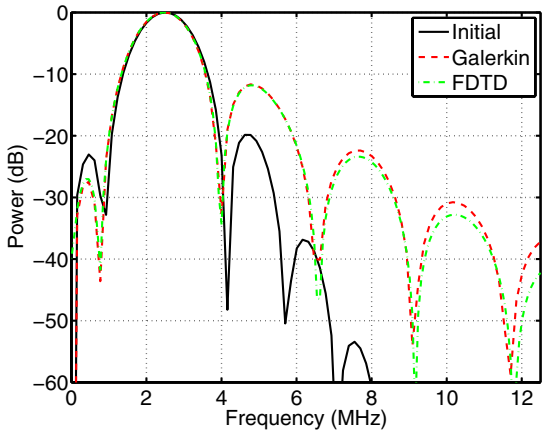

Fig. 3. Nonlinear propagation of a plane wave as calculated by the FDTD nonlinear full-wave algorithm and the Galerkin scheme. A time domain waveform is shown on the left and the power spectrum is shown on the right.

B. Experimental verification

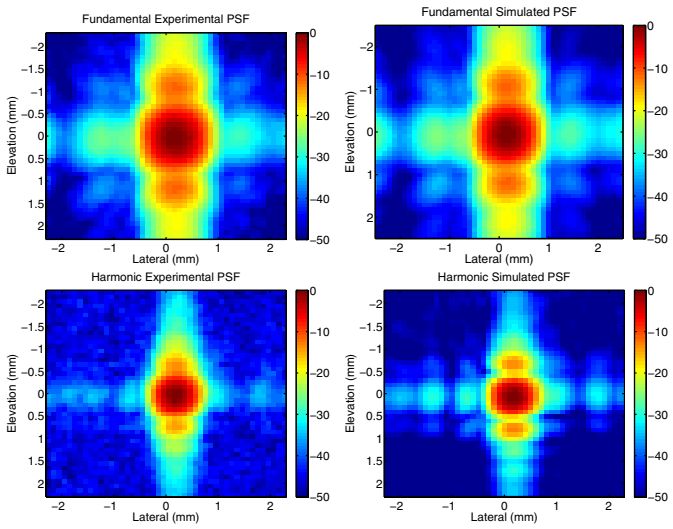

Fig. 4. Experimental (left) and simulated (right) PSF's for the fundamental (top) and harmonic (bottom) beams.

The acoustic plane at the transducer face was measured and used as an input to the full-wave simulation with the acoustic properties of water. Shown on the left of Fig 4 are the experimentally measured point spread functions for the fundamental (top) and harmonic (bottom) fields. The equivalent plots are shown for the simulated data with the experimentally determined intial conditions on the right.

There is an excellent agreement betweent the experimental and simulated fundamental PSF's in terms of primary and secondary features. The size and position of the mainlobe are very similar and the initial off-plane position of the transducer is apparent in the measured and simluated data sets. The elevation and lateral sidelobes also have similar position and amplitude. Features that are less than 35 dB down from the peak or off axis with respect the lateral and elevation planes exhibit a close correspondence even though there is a visible amount of noise in the experimental data.

The harmonic PSF's shown in the bottom of Fig. 4 have similar primary features and many of the secondary features are distinguishable even though the noise floor of the experimental data limits the accuracy of the comparison in the sub -30 dB range.

C. Ultrasonic imaging

A focused ultrasonic pulse was propagated through a two dimensional hetergeneous tissue model with twelve point scatterers per resolution.The tissue representation was obtained from a histologically stained sample of human abdominal wall [5], [3] and the structures in the tissue were correlated with their measured properties of which the speed of sound is shown on the right of Fig. 5..

A circular anechoic region with a 5 mm diameter was placed at the focus to mimic a lesion. To simulate an ultrasonic

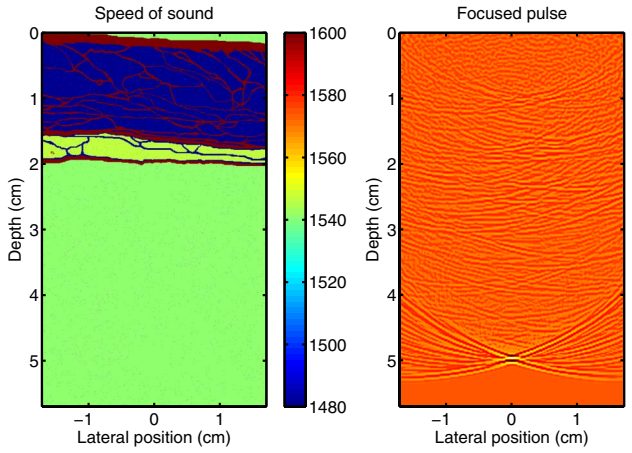

Fig. 5. On the left, a graphical representation of the variation in the speed of sound for the abdominal layer (not shown are spatial variations in attenuation, nonlinearity, and density). On the right, the acoustic field of a diagnostic pulse at the focus (scale is compressed to emphasize small amplitudes).

imaging system, a focused pulse was transmitted and allowed to propagate. The resulting reflections were measured and a standard constant F-number delay and sum beamforming algorithm was used to create a single A-line. The process was repeated by translating the transducer and forming a series of A-lines that are shown as fundamdental (left) and harmonic (right) B-mode images in Fig. 6.

IV. Conclusion

We have introduced a finite difference time domain algorithm that solves the nonlinear attenuating full-wave equation in three spatial dimensions. The numerical method propagates nonlinear diagnostic ultrasound waves in an heterogeneous attenuating medium with boundary conditions that reduce reflections to negligble levels. The entire acoustic field is simulated so the effects of reflection, reverberation, multiple scattering, and clutter can be accurately modeled and an arbitrary acoustic source can be placed anywhere in the three dimensional simulated field. In the simulations presented heterogeneities in the nonlinearity, attenuation, density, and speed of sound can be modeled with a resolution of 12.5 μm.

The numerical solutions were verified extensively. Diffraction, or the linear wave term, was verified with Field II, a simulation package that is considered a standard in linear transducer modeling, and with water tank measurements. Differences between the two simulations were less than 0.3 dB across the considered acoustic field. The nonlinear propagation was also verified numerically with results from the Galerkin method for a propagating plane wave and were shown to be agreement to within 2.5 dB up to four times the fundamental frequency. There is negligible disagreement if only the fundamental and harmonic frequencies are considered.

We demonstrated the code's ability to propagate sound through heterogeneous media by transmitting an ultrasound pulse through a measured representation of human abdominal wall. The method's capabilities were demonstrated by creating

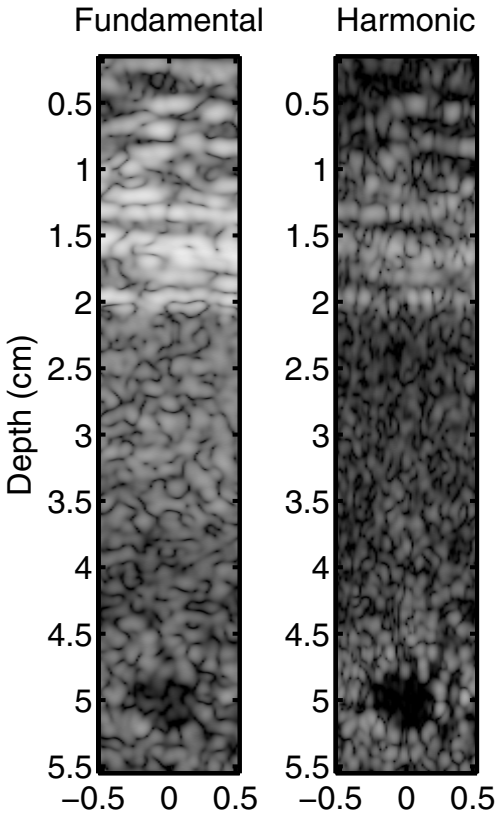

Fig. 6. Simulated fundamental (left) and harmonic (right) ultrasound images of an anechoic region below an abdominal using a transmit-receive beamformation process.

fundamental and harmonic ultrasonic images in silico through the same physical process used in a diagnostic scanner: a series of pulses were transmitted through a heterogenous scattering medium and the received acoustic field at the transducer plane was used in a beamforming algorithm.

Acknowledgments

We would like to thank Joshua Baker-LePain, T. Douglas Mast, Stephen Rosenzweig, and NIH grants R01-HL075485 and 1R01-CA114093.

References

[1] F. Tranquart, N. Grenier, V. Eder, and L. Pourcelot, "Clinical use of ultrasound tissue harmonic imaging," *Ultrasound in Medicine and Biology*, vol. 25, no. 6, pp. 889–894, July 1999.

[2] K. Wallace, B. Robinson, M. Holland, M. Rielly, and J. Miller, "Experimental comparisons of the impact of abdominal wall aberrators on linear and nonlinear beam patterns," *2004 IEEE Ultrasonics Symposium*, vol. 2, pp. 866– 869, Aug 2004.

[3] T. D. Mast, L. M. Hinkelman, M. J. Orr, V. W. Sparrow, and R. C. Waag, "Simulation of ultrasonic pulse propagation through the abdominal wall," *Journal of the Acoustical Society of America*, vol. 102, no. 2, pp. 1177–1190, Aug 1997.

[4] J. C. Strickwerda, *Finite Difference Schemes and Partial Differential Equations*. Wadsworth and Brooks/Cole, 1989.

[5] L. M. Hinkelman, D. Liu, L. A. Metlay, and R. C. Waag, "Measurements of ultrasonic pulse arrival time and energy level variations produced by propagation through abdominal wall," *J. Acoust. Soc. Am.*, vol. 95, pp. 530–541, 1994.